

# Deep Reinforcement Learning for Autonomous Ground Vehicle Exploration Without A-Priori Maps

Shathushan Sivashangaran and Azim Eskandarian, *Senior Member, IEEE*

**Abstract**—Autonomous Ground Vehicles (AGVs) are essential tools for a wide range of applications stemming from their ability to operate in hazardous environments with minimal human operator input. Efficient and effective motion planning is paramount for successful operation of AGVs. Conventional motion planning algorithms are dependent on prior knowledge of environment characteristics and offer limited utility in information poor, dynamically altering environments such as areas where emergency hazards like fire and earthquake occur, and unexplored subterranean environments such as tunnels and lava tubes on Mars. We propose a Deep Reinforcement Learning (DRL) framework for intelligent AGV exploration without a-priori maps utilizing Actor-Critic DRL algorithms to learn policies in continuous and high-dimensional action spaces, required for robotics applications. The DRL architecture comprises feedforward neural networks for the critic and actor representations in which the actor network strategizes linear and angular velocity control actions given current state inputs, that are evaluated by the critic network which learns and estimates Q-values to maximize an accumulated reward. Three off-policy DRL algorithms, DDPG, TD3 and SAC, are trained and compared in two environments of varying complexity, and further evaluated in a third with no prior training or knowledge of map characteristics. The agent is shown to learn optimal policies at the end of each training period to chart quick, efficient and collision-free exploration trajectories, and is extensible, capable of adapting to an unknown environment with no changes to network architecture or hyperparameters.

## I. INTRODUCTION

Autonomous Ground Vehicles (AGVs) are indispensable tools for mapping uncharted terrain, search & rescue missions, disaster response, military operations, mining, and extraterrestrial planetary exploration owing to their ability to operate in hazardous, unstructured environments reliably with minimal input from a human operator. Conventional AGV navigation algorithms are dependent on specific environmental configurations [1] which limits their effectiveness in adapting to dynamically changing environments such as areas where emergency hazards like fire and earthquake occur, and unexplored subterranean environments such as tunnels, caves and lava tubes on Mars.

Recent advancements in Artificial Intelligence (AI), sensors, communication and computer technology facilitate intelligent AGVs capable of high autonomy. Simultaneous Localization And Mapping (SLAM) enables AGVs to simultaneously estimate vehicle state utilizing on-board sensors and construct a model of the environment the sensors perceive [2], [3]. The inclusion of LIDAR-centric SLAM in the

perception pipeline is a key enabler for AGV navigation in environments that are GPS-denied with no access to a-priori maps [4].

Mobile robot trajectories require optimization for shortest path, minimum energy consumption and training time [5]. Conventional motion planning algorithms offer limited utility in information poor, dynamically altering environments. These comprise graph search algorithms such as Dijkstra, A\* and D\* [6] that are well-defined and simple to use but are inefficient in complex, dynamic environments and have poor robustness to noise interference and errors in the environment model, random sampling algorithms such as Probability Graph Method (PGM) and Rapid exploration Random Tree (RRT) [7] that select random scatter points in the entire environment space to search for the optimal path between the starting and end points making them susceptible to poor real-time performance, sub-optimal solutions and high computation cost, Artificial Potential Field (APF) [8] that has low computation cost and is efficient but prone to local minima traps, and nature inspired algorithms such as fuzzy logic that is robust, but requires prior knowledge in the form of user defined knowledge based logic and rules, and Genetic Algorithm (GA) [9] which is ideal for the global optimal solution and suitable for complex problems, but has poor local search ability and slow convergence rate.

Motion planning models that incorporate Artificial Neural Networks (ANN) and Actor-Critic Reinforcement Learning (RL) enable robotic systems to learn optimal, end-to-end policies in continuous and high-dimensional action spaces directly from characteristics of high-dimensional sensory input data to intelligently select goal driven actions in dynamically changing, obstacle filled unstructured terrain in the absence of prior knowledge and detailed maps [10]–[13].

On-policy Actor-Critic Deep Reinforcement Learning (DRL) algorithms such as Trust Region Policy Optimization (TRPO) [14] and Proximal Policy Optimization (PPO) [15] are robust to hyperparameter tuning and straightforward to implement, but are sample inefficient as these require new training samples for every policy update, which makes learning an effective policy for complex tasks computationally exorbitant. Off-policy Actor-Critic DRL algorithms such as Deep Deterministic Policy Gradient (DDPG) [16], Twin Delayed Deep Deterministic Policy Gradient (TD3) [17] and Soft Actor-Critic (SAC) [18] reuse past experience for learning, thus have good sample efficiency.

Given the potential of DRL for AGV navigation in information poor environments, this paper presents and evaluates a DRL architecture for intelligent AGV navigation, and

*Corresponding author: Shathushan Sivashangaran*

The authors are with the Autonomous Systems and Intelligent Machines Laboratory, Virginia Tech, Blacksburg, VA 24061, USA. (email: shathushansiva@vt.edu; eskandarian@vt.edu).

compares state-of-the-art off-policy DRL algorithms’ ability to safely navigate and explore obstacle filled terrain without prior knowledge of environment characteristics. Moreover, this paper answers research questions related to effective policy transfer between environments, and sheds light on the importance, and benefits of simulation training for complex DRL tasks. These questions are answered through multiple simulations and analyses of learning and post-training performances in environments of varying complexity.

## II. BACKGROUND ON DEEP REINFORCEMENT LEARNING

RL is a Machine Learning (ML) framework inspired by trial-and-error animal learning to train agents that interact with the surrounding environment by promoting or discouraging actions utilizing reward feedback signals designed to gauge effectiveness of executed actions. Deep Learning (DL), a key ML component, utilizes ANNs to form an abstract, distinguishable high-level representation from low-level input features. Deep Reinforcement Learning (DRL) algorithms combine DL and RL to extract unknown environment features from high-dimensional input data utilizing ANNs, and decide control actions using RL. Figure 1 portrays the DRL framework.

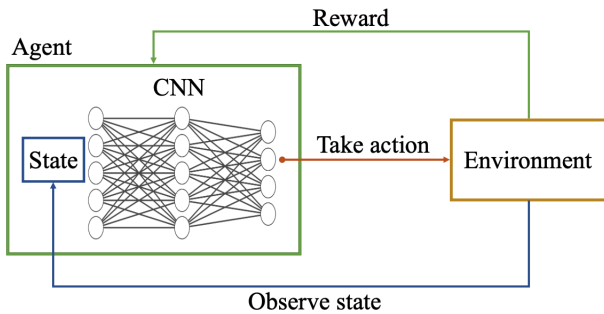


Fig. 1. Schematic of deep reinforcement learning framework.

A RL agent observes its state  $s_i$  at each time step  $t$ , and selects an action  $a_i$  from action space  $A$ , conforming to a learned policy  $\pi(a_i | s_i)$  that maps states to actions. The expectation of a discounted, accumulated reward  $R_i = \sum_{k=0}^{\infty} \gamma^k r w_{i+k}$  at each state is maximized during learning, where  $\gamma \in (0,1]$  is the discount factor, and  $r w_i$  is the scalar reward signal for selecting action  $a_i$  [19].

### A. Actor-Critic Framework

An actor-critic framework utilizing deep function approximators that combines both value-based and policy-based RL is the preferred method to learn policies in continuous and high-dimensional action spaces, required for robotics applications. This method leverages the joint computing and decision-making abilities of the actor and critic neural networks to yield low variance and fast speeds when updating gradients. Figure 2 illustrates the Actor-Critic framework.

The actor network strategizes an action output selected from a continuous action space using policy gradient, utilizing the current state as the input. The critic evaluates

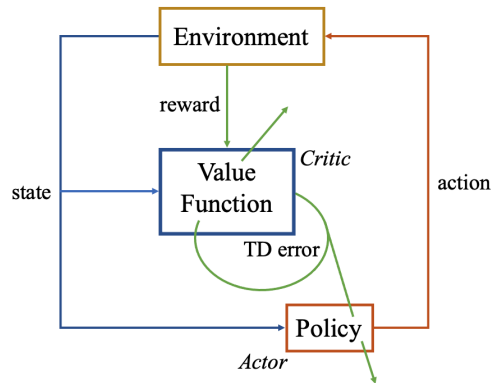


Fig. 2. Schematic of Actor-Critic framework.

the chosen actions and outputs the associated approximate Q-value for the current state and selected action using an approximated value function to counter the large variance in the policy gradients. In off-policy algorithms, sample data accumulated in a replay buffer is utilized to update and approximate the value function yielding higher sample efficiency than on-policy algorithms. The two networks compute the action prediction for the current state at each time step to generate a temporal-difference error signal.

### B. Deep Deterministic Policy Gradient

DDPG is a model-free, off-policy actor-critic RL algorithm that combines ANNs with the actor-critic representation of standard Deterministic Policy Gradient (DPG) [20] to successfully implement control sequences in a continuous action space. The actor,  $\pi(s | \theta)$  and critic,  $Q(s, a | \phi)$  each comprise fully-linked, two-layer feedforward ANNs with a Rectified Linear Unit (ReLU) activation function.

The loss  $L$  is minimized across all sampled experiences to update the critic parameters,  $\phi$ ,

$$L = \frac{1}{M} \sum_{i=1}^M (y_i - Q(s_i, a_i | \phi))^2 \quad (1)$$

Here  $M$  is a random mini-batch of experiences, and  $y_i$  is the target value function computed as follows,

$$y_i = R_i + \gamma Q_t(s_{i+1}, \pi_t(s_{i+1} | \theta_t) | \phi_t) \quad (2)$$

$\theta_t$  and  $\phi_t$  are parameters of the target actor  $\pi_t$  and target critic  $Q_t$  respectively, that have the same structure and parameterization as  $\pi$  and  $Q$ . The agent periodically updates  $\theta_t$  and  $\phi_t$  using the latest  $\theta$  and  $\phi$  values to improve the stability of the optimization.

The actor parameters,  $\theta$  are updated using a sampled policy gradient  $\nabla_{\theta} J$  to maximize the expected discounted reward,

$$\nabla_{\theta} J \approx \frac{1}{M} \sum_{i=1}^M G_{ai} G_{\pi i} \quad (3)$$

Here  $G_{ai}$  is the gradient of the critic output with respect to the action selected by the actor network computed as follows,

$$G_{a_i} = \nabla_a Q(s_i, \pi(s_i | \theta) | \phi) \quad (4)$$

$G_{\pi_i}$  is the gradient of the actor output with respect to its parameters,

$$G_{\pi_i} = \nabla_{\theta} \pi(s_i | \theta) \quad (5)$$

### C. Twin-Delayed Deep Deterministic Policy Gradient

TD3 is designed to improve learned policies by preventing overestimation of the value function. Two Q-value functions are learned simultaneously, and the minimum is used for policy updates. Moreover, the policy is updated less frequently than the Q-value function to further improve learned policies.

The parameters of the critic,  $Q_k(s, a | \phi_k)$ , where  $k = 2$  is the number of critics, are updated by minimizing the loss  $L_k$  as follows,

$$L_k = \frac{1}{M} \sum_{i=1}^M (y_i - Q_k(s_i, a_i | \phi_k))^2 \quad (6)$$

The target value function  $y_i$  is computed as follows,

$$y_i = R_i + \gamma \min_k (Q_{tk}(s_{i+1}, \text{clip}(\pi_t(s_{i+1} | \theta_t) + \varepsilon) | \phi_{tk})) \quad (7)$$

Here  $\theta_t$  and  $\phi_{tk}$  are parameters of the target actor  $\pi_t$  and target critics  $Q_{tk}$ , and  $\varepsilon$  is noise added to the computed action to promote exploration. The action is clipped based on the noise limits.

The actor parameters are updated similar to DDPG using Equation (3) where  $G_{a_i}$  is computed as follows and  $G_{\pi_i}$  is computed as in Equation (5).

$$G_{a_i} = \nabla_a \min_k (Q_k(s_i, \pi(s_i | \theta) | \phi)) \quad (8)$$

### D. Soft Actor-Critic

SAC, similar to DDPG and TD3, is a model-free, off-policy actor-critic RL algorithm. In addition to maximizing the long-term expected reward, SAC maximizes the entropy of the policy, which is a measure of the policy uncertainty at a given state. A higher policy entropy promotes exploration, hence the learned policy balances exploitation and exploration of the environment.

The agent utilizes a stochastic actor that outputs mean and standard deviation, using which an unbounded action is randomly selected from a Gaussian distribution. The entropy of the policy is computed during training for the given observation using this unbounded probability distribution. Bounded actions that comply with the action space are generated from the unbounded action by applying *tanh* and scaling operations.

The critic parameters are updated at specific time step periods by minimizing the loss function in Equation (6), similar to TD3 for  $k$  critics.

The target value function  $y_i$  is computed as the sum of the minimum discounted future reward from the critic networks  $R_i$ , and the weighted entropy as follows,

$$y_i = R_i + \gamma \min_k (Q_{tk}(s_{i+1}, \pi(s_{i+1} | \theta) | \phi_{tk})) - \alpha \ln \pi(s_{i+1} | \theta) \quad (9)$$

Here  $\alpha$  is the entropy loss weight. The entropy weight is updated by minimizing the loss function,  $L_{\alpha}$  where  $H$  is the target entropy as follows,

$$L_{\alpha} = \frac{1}{M} \sum_{i=1}^M (-\alpha \ln \pi(s_i | \theta) - \alpha H) \quad (10)$$

The stochastic actor parameters are updated by minimizing the objective function  $J_{\pi}$ ,

$$J_{\pi} = \frac{1}{M} \sum_{i=1}^M (-\min_k (Q_{tk}(s_i, \pi(s_i | \theta) | \phi_{tk})) + \alpha \ln \pi(s_i | \theta)) \quad (11)$$

## III. METHODOLOGY

This section presents the DRL architecture, reward design, training, and evaluation methodologies for collision-free AGV exploration in unknown environments. The MATLAB Robotics System [21] and Reinforcement Learning [22] Toolboxes, and Simulink are utilized to model the AGV, and train the DRL agent.

### A. Network Architecture

In order to maximize the long-term reward, designed to encourage quick, efficient, and collision-free exploration of the environment, the DRL agent makes strategic linear and angular velocity action decisions for the current time step,  $v_t$  and  $\omega_t$ . These decisions are based on LiDAR range measurements  $r$ , the AGV's state  $s = (x, y, \psi)$ , the previous time step's action  $a = (v, \omega)$ , and the corresponding reward value,  $R$ . The proposed DRL architecture for AGV exploration is shown in Figure 3.

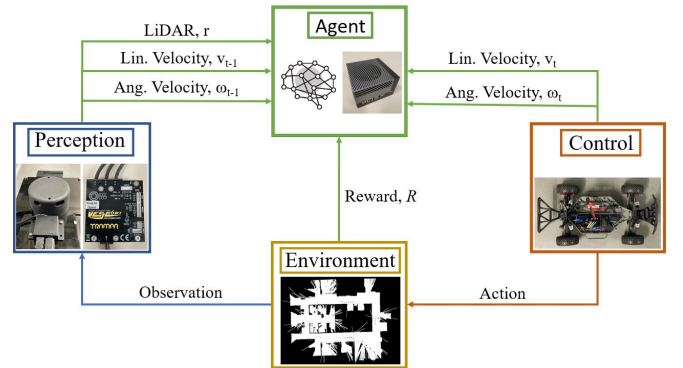


Fig. 3. Ubiquitous Deep Reinforcement Learning architecture for Autonomous Ground Vehicle exploration.

### B. Reward Function

The reward function is designed to encourage the agent to explore its environment efficiently, quickly and safely, without collisions. It computes a scalar reward value as follows,

$$R = 0.005r^2 + 1.3v^2 - 0.5\omega^2 \quad (12)$$

A positive reward is applied to the square of the minimum measurement obtained by the LiDAR sensor,  $r$  to incentivize obstacle avoidance. This reward is highest when the agent is at a greater distance from obstacles, encouraging the generation of paths devoid of obstacles. The agent is additionally rewarded for swift navigation through positive reinforcement of linear velocity,  $v$ . To encourage efficient exploration, a negative reward is applied to angular velocity,  $\omega$  to discourage repeated circular motion in the same vicinity. High coefficients for  $r^2$  and  $v^2$  lead to a compromise between obstacle avoidance ability and exploratory behavior, hence an optimal balance was determined through experimentation to prioritize both exploration, and collision avoidance.

### C. AGV Model

XTENTH-CAR [23], a proportionally scaled experimental vehicle platform, designed with similar hardware and software architectures as the full-size X-CAR [24] connected autonomous vehicle, is modeled and trained in simulation. The XTENTH-CAR AGV, shown in Figure 4, has a wheelbase of 0.32 m and utilizes the Ackermann steering mechanism.

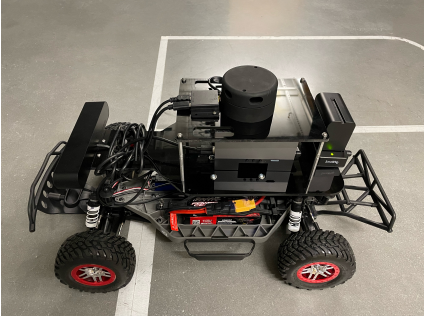


Fig. 4. XTENTH-CAR Ackermann steered AGV platform.

The AGV's kinematics are computed using a bicycle model, portrayed in Figure 5, where the front and rear wheels are represented by a single wheel located at the center of each axle. This model is accurate for use at low speeds and offers a good balance between model accuracy and computation cost [25] for evaluation of the DRL agent.

The bicycle model is represented by the following equations,

$$\dot{x} = v \cos(\psi + \beta) \quad (13)$$

$$\dot{y} = v \sin(\psi + \beta) \quad (14)$$

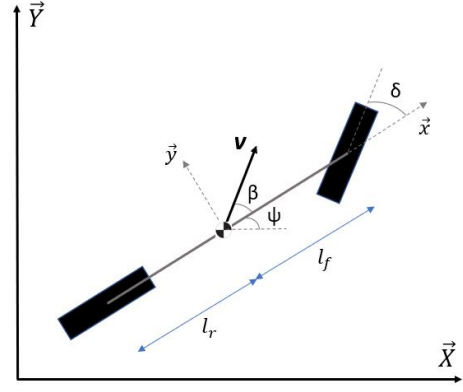


Fig. 5. Schematic of kinematic bicycle model.

$$\dot{\psi} = \frac{v}{l_r} \sin(\beta) \quad (15)$$

$$\beta = \tan^{-1} \left( \frac{l_r}{l_f + l_r} \tan(\delta) \right) \quad (16)$$

Here  $x$  and  $y$  are position coordinates of the AGV's center of mass,  $\psi$  is the angle of the AGV's heading with respect to the inertial reference frame,  $\beta$  is the angle between the velocity vector of the AGV's center of mass and its longitudinal axis,  $l_f$  and  $l_r$  are distances from the center of mass to the front and rear axles respectively, and velocity,  $v$  and steering angle,  $\delta$  are control inputs.

### D. Environments for Training and Evaluation

The DRL agent is trained in two distinct environments of varying complexity. The first environment, depicted in Figure 6, is a 25 m x 25 m space with walls that the agent must steer clear of. The second environment, illustrated in Figure 7, is a more complex 40 m x 40 m space with walls and various obstacles, marked in black, that the agent must additionally avoid.

The AGV, identified with a red symbol on the training maps, is set to a random starting position at the start of each training episode to enhance policy learning. This reset ensures that the agent is not biased towards any particular initial location.

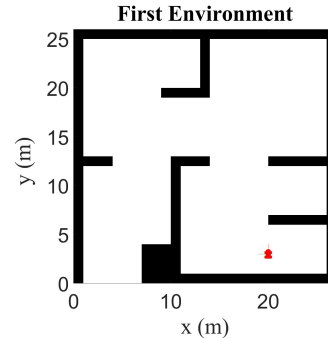


Fig. 6. First training environment with DRL agent marked in red at a randomized initial location.

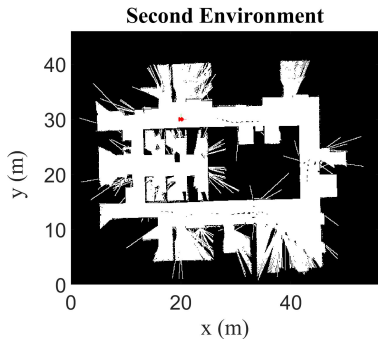


Fig. 7. Second training environment with DRL agent marked in red at a randomized initial location.

The trained agent is evaluated in a third environment, illustrated in Figure 8 to evaluate the robustness, and performance of the learned policy in a new, unknown environment with the same network architecture and hyperparameters.

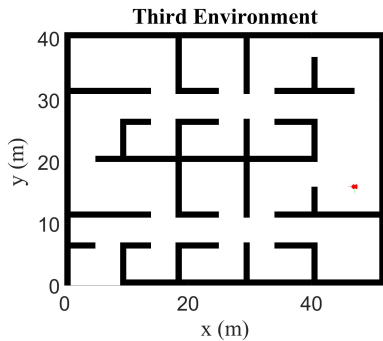


Fig. 8. Evaluation environment with DRL agent marked in red at a randomized initial location.

### E. Training Conditions and Hyperparameters

A training episode is concluded when the agent encounters an obstacle or completes the maximum number of steps permitted in a single episode. Subsequently, the agent is reset to a randomly determined starting location to initiate the next episode. The DRL agent is trained to a total of 10,000 episodes, each with a maximum of 1000 steps in the first environment, and 20,000 episodes, each with a maximum of 2000 steps in the second, to facilitate rapid iterative learning. Modified hyperparameters with non-default values are listed in Table I.

TABLE I  
NON-DEFAULT HYPERPARAMETERS

Hyperparameter	Value
Discount Factor ( $\gamma$ )	0.995
Actor Learn Rate	0.00005
Critic Learn Rate	0.0005
Target Smooth Factor	0.001
Mini Batch Size	128
Experience Buffer Length	1,000,000

## IV. RESULTS AND DISCUSSION

In this section, we present DRL training results, including post-training exploration trajectories and corresponding average return and steps achieved by the agent each episode iteration during the training period, utilizing DDPG, TD3 and SAC algorithms. We further evaluate each trained policy in a new environment with no prior knowledge of environment characteristics.

### A. Training Results

An Intel i7 11700K CPU and GeForce RTX 3070 Ti GPU were used for training. Table II summarizes the training times for each DRL algorithm in the evaluated environments.

TABLE II  
TRAINING TIMES

Case	Training Time (Hrs)
First Environment: DDPG	66.0
First Environment: TD3	95.3
First Environment: SAC	156.7
Second Environment: DDPG	84.8
Second Environment: TD3	128.1
Second Environment: SAC	203.9

SAC required the longest training time, followed by TD3 and DDPG which required the least. On average, training in the second, more complex environment required 31% longer training time than in the first, over twice the number of training episodes. DDPG required 28.5%, TD3 34.4% and SAC 30.1% longer to train in the second environment.

In the first environment, TD3 required 44.4% longer to train than DDPG, and SAC 137.4% longer than DDPG and 64.4% longer TD3. In the second environment, TD3 required 51.1% longer to train than DDPG, and SAC 140.4% longer than DDPG and 59.2% longer than TD3. On average, TD3 required 47.8% longer training time than DDPG, and SAC 138.9% longer than DDPG and 61.8% longer training time than TD3.

Training times ranged from 2.75 days in the first environment for DDPG to 8.5 days in the second environment for SAC. More optimal policies require longer training times to accommodate increased episode steps in the first environment, and more training episodes in the second.

1) *First Environment*: The order 50 moving average return and agent steps during training in the first environment are illustrated in Figures 9 and 10. The training results in the first environment are summarized in Table III.

DDPG converges first at 170 episodes with an average return of 318 and 865 average steps. TD3 converges last at 960 episodes with an average return of 435 and 1000 average steps, and SAC converges at 390 episodes with an average return of 320 and the maximum 1000 average steps.

DDPG learned the least optimal policy with the lowest average return and agent steps. TD3 achieves the highest return, and the maximum 1000 steps, however SAC achieves

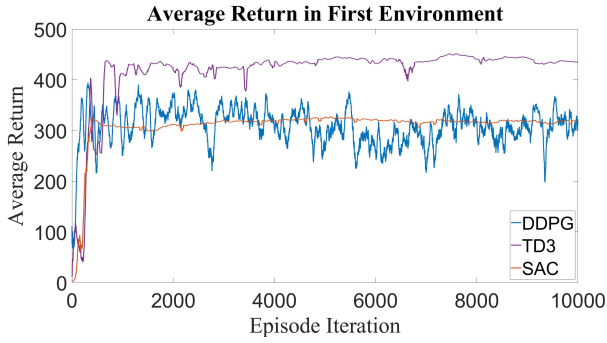


Fig. 9. Order 50 moving average return during training in the first environment.

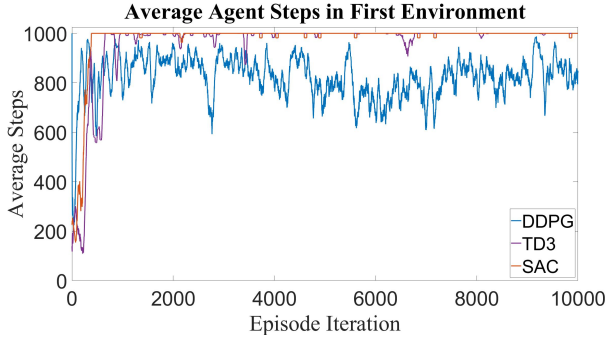


Fig. 10. Order 50 moving average agent steps during training in the first environment.

1000 exploration steps more consistently post training convergence. Unlike TD3 which solely maximizes the long-term expected reward, SAC additionally maximizes the entropy of the policy to promote exploration. Consequently, TD3 learns a policy with a higher return, but SAC learns the better policy for agent exploration.

The trajectories in the first environment for each algorithm after the first training episode are illustrated in Figure 11.

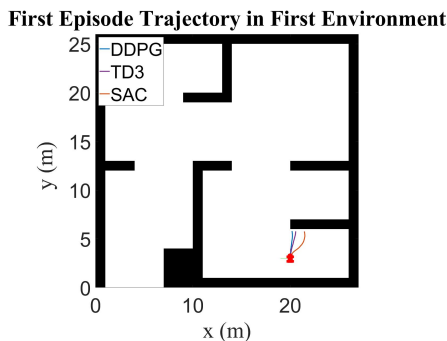


Fig. 11. Trajectories in the first environment post first training episode.

All three agents collide having no prior training experience. SAC covers the most ground after one training episode.

The trajectories in the first environment for each algorithm post training completion are illustrated in Figure 12.

Each algorithm achieves 1000 episode steps without collision. SAC covers the most ground, and exhibits the most efficient exploratory behavior which will result in the greatest energy savings. TD3 is next best, followed by DDPG which

TABLE III  
FIRST ENVIRONMENT TRAINING RESULTS

Algorithm	Convergence Episode	Average Return	Average Agent Steps
DDPG	170	318	865
TD3	960	435	1000
SAC	390	320	1000

Post-Training Trajectory in First Environment

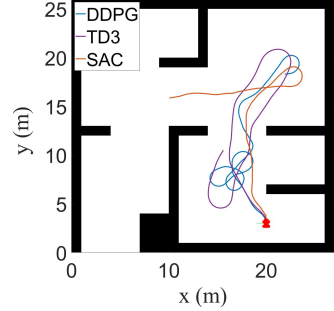


Fig. 12. Trajectories in the first environment post training completion.

is the most inefficient, covering the same region multiple times.

2) *Second Environment*: The order 50 moving average return and agent steps during training in the second environment are illustrated in Figures 13 and 14. The training results in the second environment are summarized in Table IV.

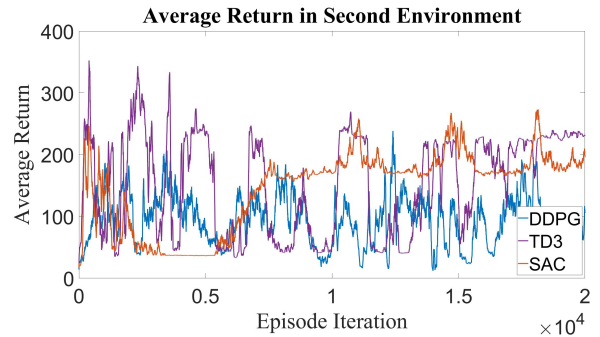


Fig. 13. Order 50 moving average return during training in the second environment.

Training for 20,000 episodes is insufficient for the DRL algorithms to learn an optimal policy in the second environment. At the end of the training period, DDPG achieves an average return of 125 and 530 average steps, TD3 obtains an average return of 230 and 715 average steps, and SAC converges to a local maximum at 10,620 episodes with an average return of 210 and 1050 average steps. Training was limited to 20,000 episodes to gauge performance in a reasonable time frame, however, continued training over 75,000 to 100,000 episodes will enable the agents to learn an optimal policy to traverse the more complex terrain over an indefinite number of exploration steps.

Training DDPG, TD3 and SAC algorithms in the second

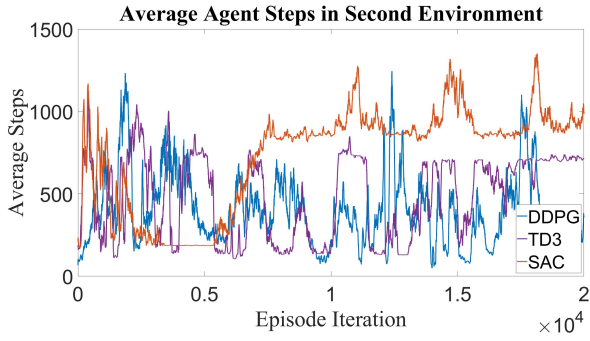


Fig. 14. Order 50 moving average agent steps during training in the second environment.

TABLE IV  
SECOND ENVIRONMENT TRAINING RESULTS

Algorithm	Average Return	Average Agent Steps
DDPG	125	530
TD3	230	715
SAC	210	1050

environment for 20,000 episodes required a total of 416.8 hours, as such, it is infeasible to evaluate the algorithms for 75,000+ episodes with the existing setup. More powerful computer hardware is required. Similar to the training results in the first environment, DDPG learned the least optimal policy achieving the lowest return and agent steps. TD3 achieved the highest return, however SAC learned a more optimal policy achieving the highest agent steps.

The trajectories in the second environment for each algorithm after the first training episode are illustrated in Figure 15.

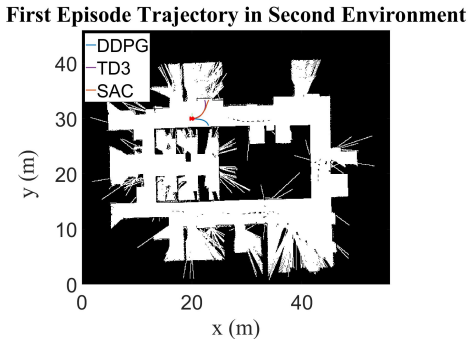


Fig. 15. Trajectories in the second environment post first training episode.

DDPG covers the least ground after one training episode. SAC and TD3 cover a similar distance. All three agents collide after travelling a short distance with no prior training experience.

The trajectories in the second environment for each algorithm post training completion are illustrated in Figure 16.

SAC achieves the best performance, learning a trajectory that covers the most distance. TD3 and DDPG yield similar performance, with TD3 being a marginal improvement.

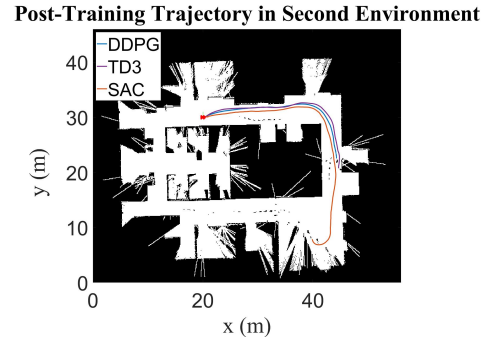


Fig. 16. Trajectories in the second environment post training completion.

### B. Trained Policy Evaluation

The six agents, DDPG, TD3 and SAC, trained in two different environments are evaluated in a third unknown environment with no prior training or knowledge of environment characteristics, to evaluate the extensibility of the ubiquitous DRL architecture for AGV exploration in information poor environments. Figure 17 portrays the trajectories for each agent in the third environment. The evaluation results are summarized in Table V.

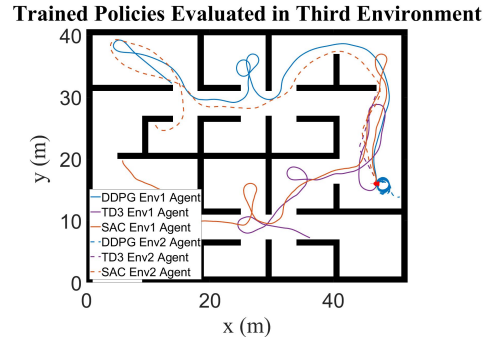


Fig. 17. Trained DRL agents evaluated in the third environment.

TABLE V  
THIRD ENVIRONMENT EVALUATION RESULTS

Agent	Agent Steps
DDPG Env1	2151
TD3 Env1	1533
SAC Env1	2971
DDPG Env2	2893
TD3 Env2	321
SAC Env2	2839

The SAC agents demonstrate the best performance, covering the most ground, efficiently. The DDPG agent trained in the first environment covers more ground than either TD3 agent, however is more inefficient. DDPG trained in the second environment covers the second highest distance, but yields the worst exploratory behavior, repeatedly traversing a circular trajectory in the same vicinity. TD3 agents cover less ground, and exhibit less efficient exploratory behavior

than SAC. The DRL agents trained in the first environment performed better than those trained in the second, as the characteristics of the evaluated environment are more similar to the first than the second. The SAC agents are most robust to differences in environment characteristics with both achieving near identical performance.

The reward function weights and network hyperparameters can be further engineered for this application, and the agent trained over a longer period with more episode steps each episode iteration to learn an improved policy that explores the surrounding environment indefinitely.

Bridging the simulation to reality gap to transfer policies learned in simulation to real-world robotic systems is a current area of active research. The large number of episodes required to sufficiently train the agent renders simulation training an essential component for DRL in robotics applications to minimize cost and possible physical damage caused by collisions during training. Substantial computation cost is required for training, however, post-training implementation of DRL agents is significantly less expensive, which makes DRL a powerful tool for real-time AGV motion planning and control in environments without a-priori maps.

## V. CONCLUSIONS

This paper presented an ubiquitous DRL architecture for intelligent AGV exploration without a-priori maps. Three actor-critic DRL algorithms, DDPG, TD3 and SAC, were trained in two environments of varying complexity, and further evaluated in a third with no prior knowledge of map characteristics. Simulation results demonstrate the effectiveness of the proposed DRL architecture, reward function and training conditions for quick, efficient and collision-free AGV navigation. SAC achieves the best performance, yielding trajectories that cover the highest distance, and demonstrate the most efficient exploratory behavior. Learning requires substantial computation cost, requiring up to 8.5 days for SAC in the second, complex environment using an Intel i7 11700K CPU and GeForce RTX 3070 Ti GPU. Improved policies with higher post-training episode steps require greater training times. Despite the high training cost, post-training implementation of DRL agents is significantly less expensive, which makes DRL a powerful tool for real-time AGV exploration in information poor, dynamically altering environments. For future work, the simulation to reality gap will be bridged to transfer policies learned in simulation to the physical AGV.

## REFERENCES

- [1] J. Levinson, J. Askeland, J. Becker, J. Dolson, D. Held, S. Kammel, J. Z. Kolter, D. Langer, O. Pink, V. Pratt *et al.*, "Towards fully autonomous driving: Systems and algorithms," in *2011 IEEE intelligent vehicles symposium (IV)*. IEEE, 2011, pp. 163–168.
- [2] C. Cadena, L. Carlone, H. Carrillo, Y. Latif, D. Scaramuzza, J. Neira, I. Reid, and J. J. Leonard, "Past, present, and future of simultaneous localization and mapping: Toward the robust-perception age," *IEEE Transactions on Robotics*, vol. 32, no. 6, pp. 1309–1332, 2016.
- [3] G. Bresson, Z. Alsayed, L. Yu, and S. Glaser, "Simultaneous localization and mapping: A survey of current trends in autonomous driving," *IEEE Transactions on Intelligent Vehicles*, vol. 2, no. 3, pp. 194–220, 2017.
- [4] K. Ebadi, L. Bernreiter, H. Biggie, G. Catt, Y. Chang, A. Chatterjee, C. E. Denniston, S.-P. Deschênes, K. Harlow, S. Khattak *et al.*, "Present and future of slam in extreme underground environments," *arXiv preprint arXiv:2208.01787*, 2022.
- [5] P. Victorpaul, D. Saravanan, S. Janakiraman, and J. Pradeep, "Path planning of autonomous mobile robots: A survey and comparison," *Journal of Advanced Research in Dynamical and Control Systems*, vol. 9, no. 12, pp. 1535–1565, 2017.
- [6] H. Wang, Y. Yu, and Q. Yuan, "Application of dijkstra algorithm in robot path-planning," in *2011 second international conference on mechanic automation and control engineering*. IEEE, 2011, pp. 1067–1069.
- [7] J. D. Gammell, S. S. Srinivasa, and T. D. Barfoot, "Informed rrt\*: Optimal sampling-based path planning focused via direct sampling of an admissible ellipsoidal heuristic," in *2014 IEEE/RSJ International Conference on Intelligent Robots and Systems*. IEEE, 2014, pp. 2997–3004.
- [8] P. Vadakkepat, K. C. Tan, and W. Ming-Liang, "Evolutionary artificial potential fields and their application in real time robot path planning," in *Proceedings of the 2000 congress on evolutionary computation. CEC00 (Cat. No. 00TH8512)*, vol. 1. IEEE, 2000, pp. 256–263.
- [9] A. Bakdi, A. Hentout, H. Boutami, A. Maoudj, O. Hachour, and B. Bouzouia, "Optimal path planning and execution for mobile robots using genetic algorithm and adaptive fuzzy-logic control," *Robotics and Autonomous Systems*, vol. 89, pp. 95–109, 2017.
- [10] S. Sivashangaran, "Application of deep reinforcement learning for intelligent autonomous navigation of car-like mobile robot," Master's thesis, State University of New York at Buffalo, 2021.
- [11] S. Sivashangaran and M. Zheng, "Intelligent autonomous navigation of car-like unmanned ground vehicle via deep reinforcement learning," *IFAC-PapersOnLine*, vol. 54, no. 20, pp. 218–225, 2021.
- [12] K. Zhu and T. Zhang, "Deep reinforcement learning based mobile robot navigation: A review," *Tsinghua Science and Technology*, vol. 26, no. 5, pp. 674–691, 2021.
- [13] T. N. Larsen, H. Ø. Teigen, T. Laache, D. Varagnolo, and A. Rasheed, "Comparing deep reinforcement learning algorithms' ability to safely navigate challenging waters," *Frontiers in Robotics and AI*, vol. 8, 2021.
- [14] J. Schulman, S. Levine, P. Abbeel, M. Jordan, and P. Moritz, "Trust region policy optimization," in *International conference on machine learning*. PMLR, 2015, pp. 1889–1897.
- [15] J. Schulman, F. Wolski, P. Dhariwal, A. Radford, and O. Klimov, "Proximal policy optimization algorithms," *arXiv preprint arXiv:1707.06347*, 2017.
- [16] T. P. Lillicrap, J. J. Hunt, A. Pritzel, N. Heess, T. Erez, Y. Tassa, D. Silver, and D. Wierstra, "Continuous control with deep reinforcement learning," *arXiv preprint arXiv:1509.02971*, 2015.
- [17] S. Fujimoto, H. Hoof, and D. Meger, "Addressing function approximation error in actor-critic methods," in *International conference on machine learning*. PMLR, 2018, pp. 1587–1596.
- [18] T. Haarnoja, A. Zhou, K. Hartikainen, G. Tucker, S. Ha, J. Tan, V. Kumar, H. Zhu, A. Gupta, P. Abbeel *et al.*, "Soft actor-critic algorithms and applications," *arXiv preprint arXiv:1812.05905*, 2018.
- [19] R. S. Sutton and A. G. Barto, *Reinforcement learning: An introduction*. MIT press, 2018.
- [20] D. Silver, G. Lever, N. Heess, T. Degris, D. Wierstra, and M. Riedmiller, "Deterministic policy gradient algorithms," in *International conference on machine learning*. PMLR, 2014, pp. 387–395.
- [21] The Mathworks, Inc. Robotics System Toolbox. MATLAB. Natick, Massachusetts, United States. [Online]. Available: <https://www.mathworks.com/products/robotics.html>
- [22] The Mathworks, Inc. Reinforcement Learning Toolbox. MATLAB. Natick, Massachusetts, United States. [Online]. Available: <https://www.mathworks.com/products/reinforcement-learning.html>
- [23] S. Sivashangaran and A. Eskandarian, "XTENTH-CAR: A proportionally scaled experimental vehicle platform for connected autonomy and all-terrain research," *arXiv preprint arXiv:2212.01691*, 2022.
- [24] G. Mehr, P. Ghorai, C. Zhang, A. Nayak, D. Patel, S. Sivashangaran, and A. Eskandarian, "X-CAR: An experimental vehicle platform for connected autonomy research," *IEEE Intelligent Transportation Systems Magazine*, pp. 2–19, 2022.
- [25] P. Polack, F. Althé, B. d'Andréa Novel, and A. de La Fortelle, "The kinematic bicycle model: A consistent model for planning feasible trajectories for autonomous vehicles?" in *2017 IEEE intelligent vehicles symposium (IV)*. IEEE, 2017, pp. 812–818.